Improving noise assessment at intersections by modeling traffic dynamics

E. Chevallier, A. Can, M. Nadji, L. Leclercq*

Université de Lyon
ENTPE / INRETS - Laboratoire d'Ingénierie Circulation Transport

Abstract

Three families of road noise prediction models can be distinguished depending on the way they account for traffic flow. *Static noise models* only consider free-flow constant-speed traffic with uniformly distributed vehicles. *Analytic noise models* assume that all vehicles are isolated from one another but account for their mean kinematic profile over the network. *Micro-simulation noise models* relax the hypothesis of no interaction between vehicles and fully capture traffic flow dynamic effects such as queue evolution. This study compares the noise levels obtained by these three methodologies at signalized intersections and roundabouts. It reveals that micro-simulation noise models outperform the other approaches. Particularly, they are able to capture the effects of stochastic transient queues in undersaturated conditions as well as stop-and-go behaviors in oversaturated regime. Accounting for traffic dynamics is also shown to improve predictions of noise variations due to different junction layouts. In this paper, a roundabout is found to induce a 2.5dB(A) noise abatement compared to a signalized intersection in undersaturated conditions while the acoustic contributions of both kinds of junctions balance in oversaturated regime.

Keywords: urban traffic noise, signalized intersection, roundabout, traffic dynamics, traffic management, urban planning

* corresponding author, Tel.: (+33) (0)4 72 04 77 16 , e-mail: **leclercq@entpe.fr**

1. INTRODUCTION

Temporal and spatial variations in vehicle speeds have a substantial impact on traffic noise emissions. At intersections, vehicle kinematics is strongly influenced by: (i) *single vehicle dynamics* in the absence of other traffic; (ii) *traffic dynamics* induced by vehicle interactions and queue length evolution. Depending on the way noise prediction models account for traffic flow, these dynamic effects are more or less accurately captured.

In *static noise models*, roads are divided into sections where the traffic flow is considered smooth and homogeneous. Since this assumption does not hold in the vicinity of intersections, some models like the German RLS90 (RLS, 1990) include a propagation correction term. Others, such as the Nordic model (Jonasson and Storeheier, 2001) or the ASJ RTN Model (Yoshihisa et al., 2004), modify the emission law to represent the effects of transient driving conditions. Yet, the dynamic effects (i) and (ii) are just accounted for by ad-hoc empirical or statistical formula.
Other engineering national standards like the FHWA TNN model (Menge et al., 1998) or the French noise estimation model (Certu, 1980) attempt to capture the impact of interrupted traffic on the average vehicle speed profile. They split each road section into subsegments where vehicles are assumed to have a constant average velocity and homogeneous running conditions. Each subsegment is then considered as a line source whose sound power level is calculated from the average flow rate and the sound power level of a single isolated vehicle (varying with its velocity). Engineering standards can be refined by considering average vehicle kinematic patterns continuously. This is the purpose of *analytic noise models*. Mean vehicle kinematic patterns are combined to a noise emission law to compute instantaneous sound power levels due to the bypass of a single vehicle. Traffic flow only consists in vehicles driving over the road section with constant time-headways. Instantaneous sound pressure levels at a given reception point are obtained by considering each vehicle as a mobile line source. Based on this approach, a few studies attempt to derive equivalent sound pressure formula in terms of the number of freely-moving and stopping vehicles (Makarewicz et al., 1999) or the number of queuing vehicles at traffic signals (Stoilova and Stoilov, 1998). Contrary to static noise procedures, analytic models account for single vehicle dynamics (i). Thus, they are partly able to assess the noise contribution of different kind of intersections (Makarewicz and Golebiewski, 2007; Picaut et al., 2005). However, they disregard traffic dynamics (ii) induced by vehicle interactions or saturation.
At intersections, the only way to capture the noise impacts of both single vehicle dynamics and traffic dynamics is to use a *micro-simulation noise model* such as M+P JARI (Suzuki et al., 2003), MOBILEE (De Coensel et al., 2005), TUNE (Goodman, 2001), ROTRANOMO (Volkmar, 2005) or SYMUBRUIT (Leclercq and Lelong, 2001). These models are based on different microscopic traffic simulation tools which give position, speed and acceleration of each vehicle, at each instant. Those outputs are fed into a noise emission law to assign an instantaneous sound power level to each vehicle. Then, instantaneous sound pressure levels at a given reception point can be calculated with a sound propagation model.

The goal of this paper is to demonstrate that micro-simulation noise models outperform other approaches at intersections where the influence of traffic on vehicle kinematics is expected to prevail. Few studies have been conducted to assess noise level deviations resulting from the different methodologies. The comparison between a micro-simulation noise model and the static STAMINIA-NCHRPR model was performed in Wayson et al. (1997) at signalized intersections. Based on experimental data, it reveals that the static model underestimates the noise levels compared to the simulation model. De Coensel et al. (2006) derived analytical correction formula for engineering national standards to catch-up the noise deviation compared to a micro-simulation model at different kind of intersections. In the same spirit, this study will highlight the need to capture traffic dynamics to improve noise estimates, especially in oversaturated conditions. For this, emission levels produced by: (i) a static noise emission procedure; (ii) a well-established analytic noise model and (iii) a micro-simulation noise package will be compared. Both signalized intersections and roundabouts will be studied in undersaturated and oversaturated conditions.

The first part of this paper will expose the geometric layout of the studied site when it is transformed into a signalized intersection or a roundabout. Demand rates representative of a 2h-commuting period as well as kinematic parameters will also be presented. Then, a detailed description of the static, analytic and micro-simulation noise models will be performed. The second section will highlight the results of the comparison between the three models before stating some concluding remarks.

2. METHODOLOGY

2.1. Case study

2.1.1. Geometric design

The case study consists of a major road crossing a minor road with traffic demands of respectively Δ_1 and Δ_2 (see figure 1a).

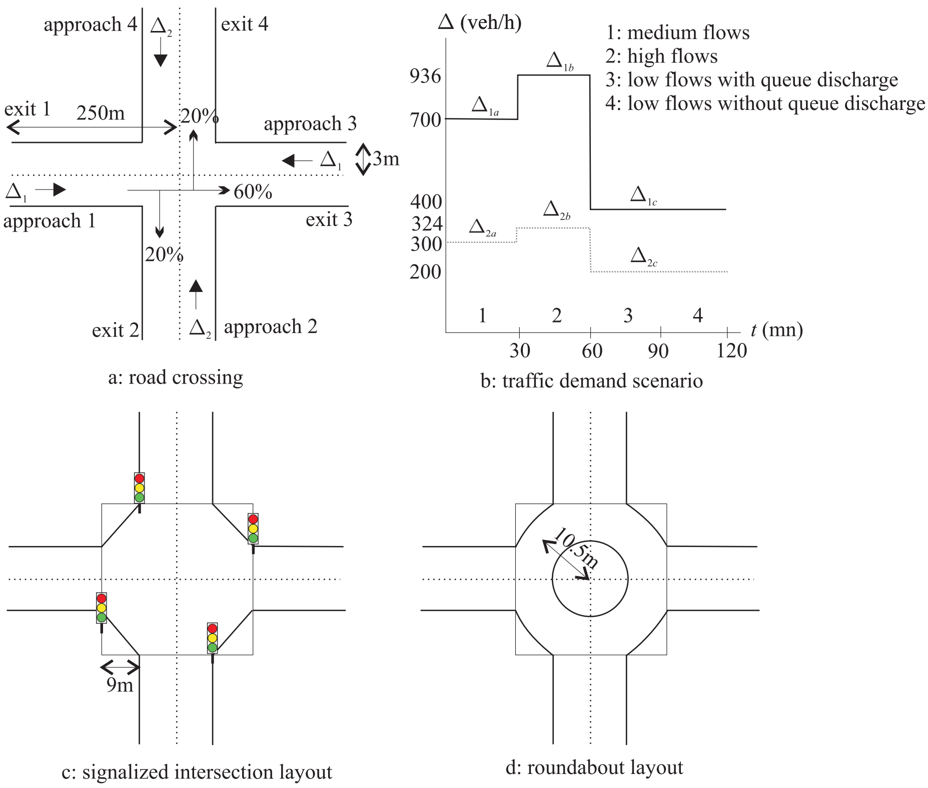

Fig.1. Case study

The four approaching and the four departure arms are one-lane sections of 3m-width. Their length is set equal to 250m since the noise impacts of road crossings can be neglected at farther distances. The signalized intersection and roundabout layouts are represented in figures 1c and 1d. They were chosen so that the stop-lines of the signalized intersection correspond to the yield-lines of the roundabout entries. The inscribed circle diameter of the roundabout is 24m and the circulatory roadway is 3m-width. At the signalized intersection, the distance between the stop line and the line extended from the edge of the intersection road is 9m. The green period G is set to 27s (respectively 16s) for the major (respectively the minor) road. The signal cycle c is equal to 55s to account for lost-times during both signal phases.

2.1.2. Demand flow scenario

The chosen demand scenario is representative of a morning commuting period. On the major (respectively the minor) road, the traffic demand pattern is a step function (see figure 1b) with three thresholds Δ_{1a}, Δ_{1b} and Δ_{1c} (respectively Δ_{2a}, Δ_{2b} and Δ_{2c}). Four different periods are separately studied in the sequel. The first 30mn-period is a free-flow period (undersaturated regime) with medium demand thresholds on both roads. The next 30mn-period is a peak period (oversaturated regime) with high demand thresholds which trigger a queue on the major road. Traffic conditions become fluid again during the next 30mn-period when the demand rates drop to low levels. Note that few minutes are required to discharge the queue before recovering free-flow conditions. Finally, the fourth 30mn-period is also a free-flow period with low demand thresholds. With this demand profile, the Highway Capacity Manual (TRB, 2000) predicts the same average delay and 95^{th}-percentile queue for both intersection types at the end of the peak period: 62s and 36 queuing vehicles on approaching arms 1 and 3; 19s and 5 queuing vehicles on approaching arms 2 and 4. This study only focuses on one category of vehicles (light-duty vehicles) to ease comparison. The origin-destination matrix is the same for each arm: 20% of traffic turns left or right; 60% goes straight ahead. In the sequel Δ_{ij} denotes the demand rate between approach i and exit j.

2.1.3. Vehicle kinematics

Vehicle kinematic parameters are chosen to match the speed profiles commonly observed at signalized intersections or roundabouts and recommended by the U.S. Federal Highway Administration (Robinson, 2000; Rodegerdts, 2004). The *free-flow speed* u on each arm is set to 54km/h. For the given roundabout geometry, the *circulatory speed* u_c (speed on the circulatory roadway) is chosen equal to a constant value of 21.2km/h. The *operating speed* u_t for turning movements at the signalized intersection is set equal to 16.6km/h. The *desired deceleration rate* d is calibrated from the FHWA stopping sight distance. For both intersection types and an initial speed of 54km/h, a value of 73m is recommended which induces an average deceleration rate of 2.6m/s^2 if a 2s-reaction time is assumed. The *desired acceleration rate* a is assumed to decrease with velocity: a=1.5m/s^2 if $v \in [0;21]$ km/h; a=1m/s^2 if $v \in [21;36]$ km/h; a=0.5m/s^2 otherwise.

2.2. Noise calculation process

2.2.1. Noise emission laws

The FHWA noise emission database (Fleming et al., 1995) is selected to characterize all light-duty vehicles. This hypothesis was chosen to adapt this study to a North American context. The maximum A-weighted sound energy level E_A due to the passby of a single vehicle at 15 meters to the side and 1.5m high depends on the velocity v (in km/h) and on throttle conditions:

$$E_A(v) = (0.6214v)^{41.7/10} 10^{1.1/10} + 10^{C/10} \quad \text{with} \quad \begin{cases} C = 50.1 \text{ for cruising throttle} \\ C = 67.0 \text{ for full throttle} \end{cases} \tag{1}$$

Sound energy levels can be converted to sound power levels L_{wn} emitted by a single vehicle n according to the following equation:

$$L_{wn} = 10\log(E_A) + 31.5 \quad \text{(in dB(A))} \tag{2}$$

Emission laws for both throttle conditions are depicted in figure 2a. The throttle conditions are specified by the acceleration rate: (i) full throttle for $a \geq 0.5\text{m/s}^2$; (ii) cruising throttle otherwise. Note that emission laws are the combination of the engine-exhaust noise which is the primary source of sound waves for speeds below 30km/h and of the tire-pavement noise.

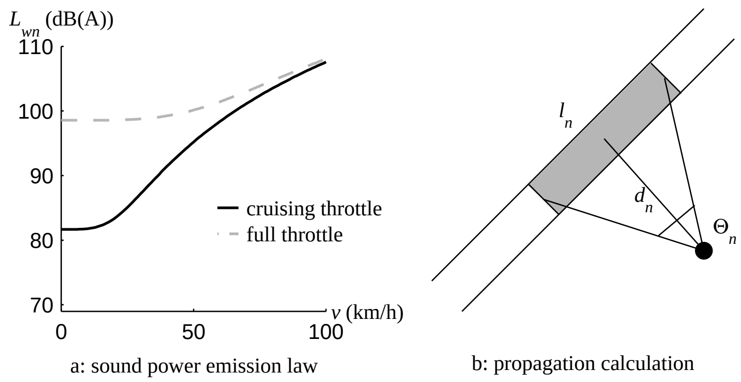

Fig.2. Noise calculation

2.2.2. Sound propagation model

The propagation model consists in calculating at each instant the noise attenuation between every vehicle on the intersection and any reception point P. In this study, the refection and diffraction effects are neglected since: (i) the goal is to compare different noise emission procedures independently of the surrounding environment; (ii) noise levels will be calculated close to the road sections.

Each vehicle n is considered as a moving line source. The attenuation due to geometrical spreading depends on its distance d_n from P, its length l_n and its angle Θ_n which vary in terms of the positions at the beginning and the end of the time-step Δt (see figure 2b). The instantaneous sound pressure level at P is given by:

$$L_{Aeq,\Delta t} = 10\log\left(\sum_n \frac{\Theta_n}{2\pi d_n l_n} 10^{\frac{L_{wn}}{10}}\right) \tag{3}$$

Note that the instantaneous sound power level of the source, L_{wn}, is directly given by the noise emission model (function of vehicle speed and acceleration).

In static and analytic noise models, vehicles are distributed over the road sections with constant time-headways equal to the inverse of the demand rate. Since this traffic flow representation is unrealistic, the time-series of $L_{Aeq,\Delta t}$ are not meaningful. On the contrary, in micro-simulation noise models, vehicles are directly output from the traffic flow simulation model which attempts to reproduce real traffic conditions. As a result, it is relevant to study the shape of the $L_{Aeq,\Delta t}$ distributions.

2.2.3. Noise descriptors used for the comparison study

The static, analytic and micro-simulation noise models will be compared in terms of the equivalent sound pressure level, $L_{Aeq,T}$ over a given period $T = m\Delta t$ ($m \in \mathbb{N}$):

$$L_{Aeq,T} = 10\log\left(\frac{1}{m}\sum_{j=1}^{m} 10^{L_{Aeq,j\Delta t}/10}\right) \quad (4)$$

Values of $L_{Aeq,T}$ will be calculated for the four 30mn-periods of the demand scenario. A set of 24 reception points along the major road is chosen. Two receptors (M_1 and M_{24}) are at 225m from the intersection center, two others (M_{12} and M_{13}) are placed between the major and the minor road. The other twenty receptors are set along the approaching and departure arms at 5m from the road axis and are 5m-spaced (see figure 3).

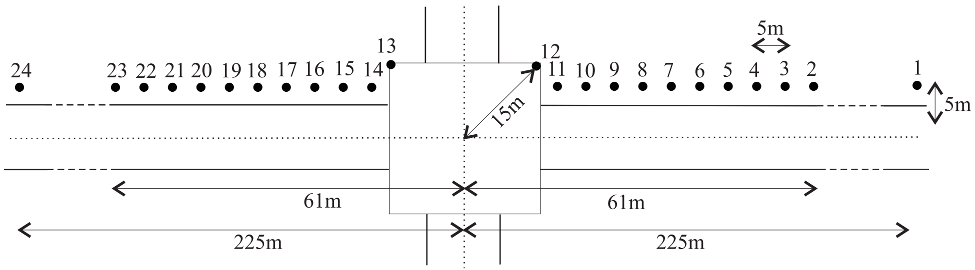

Fig.3. Location of the reception points

2.3. Traffic flow representations

In the static and analytic noise models, traffic volume between approach i and exit j is simply accounted for by distributing vehicles with time-headways equal to $1/\Delta_{ij}$. While this traffic flow representation may be acceptable for low volumes, it is inaccurate as soon as one of the approach is congested. Indeed, it disregards the drop in effective traffic flows due to the capacity constraint of the congested arm. This issue is overcome in the micro-simulation noise model which can explicitly represent oversaturated conditions.

2.3.1. Static model

In the chosen static noise model (as in all existing static noise models), the intersection impact on single vehicle dynamics is not explicitly accounted for. The operating speed on the approaching and departure sections is equal to the free-flow speed u whatever the traffic volume is. All vehicles are assumed to run on cruising conditions. The layout reduces to a set of northbound, southbound, eastbound and westbound roadways without detailing vehicle movements in the core of the intersection.

2.3.2. Analytic model

The chosen analytic model is a refinement of the FHWA TNN model (Menge et al., 1998). Instead of averaging the vehicle speed profiles per subsegment, it considers them continuously. Vehicle speeds and running conditions are given at each instant by the average kinematic patterns depicted in figure 4. They are in perfect agreement with the kinematic parameters presented in section 2.1.3. Contrary to the TNN model, speed profiles vary with the intersection type. Moreover, two modes of motion are distinguished: stopping vehicles and freely-moving vehicles which are not disturbed by vehicle interactions or traffic signal control.

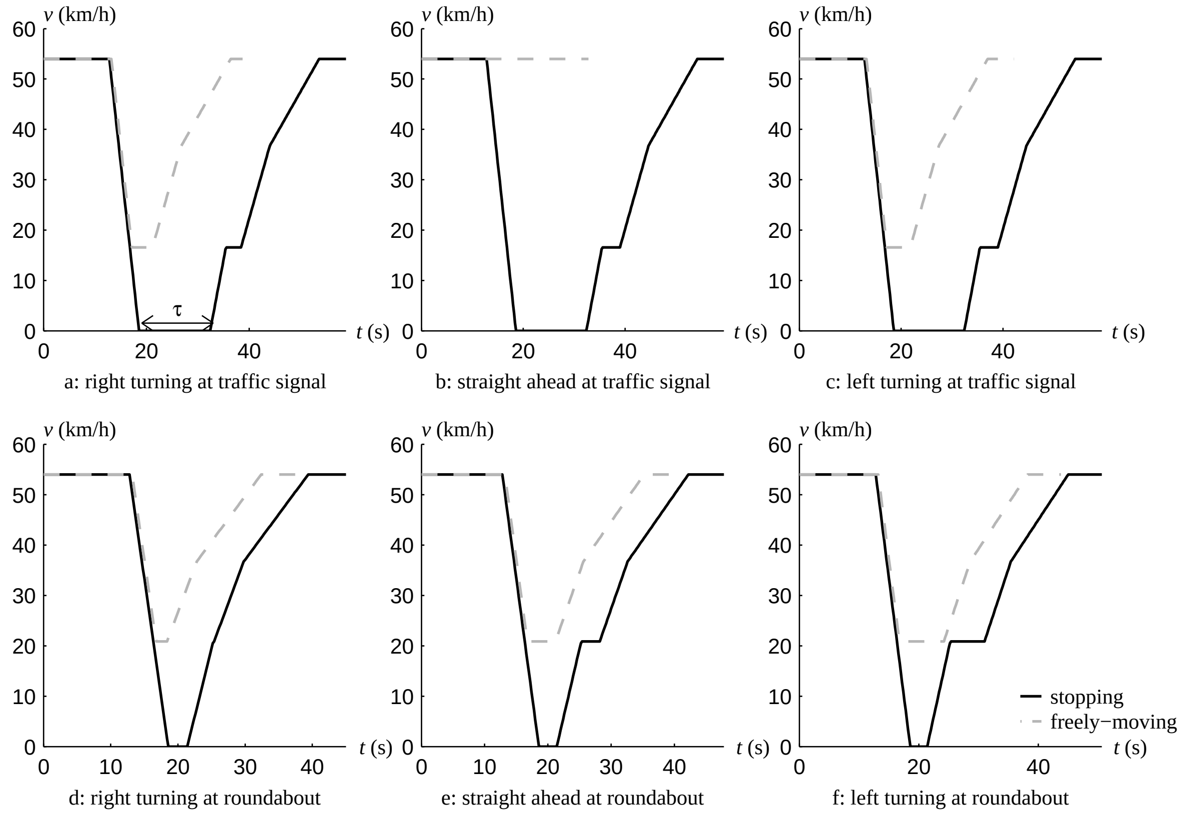

Fig.4. Average kinematic patterns used in the analytic noise model

The proportion p of stopping vehicles and the average waiting time τ at the stop or yield lines are derived from probabilistic calculation. At signalized intersections p and τ only depend on the traffic signal cycle: $p = (c - G)/c$ and $\tau = (c - G)/2$. At roundabouts they are influenced by: (i) the headway distribution and the traffic volume q_c on the circulatory roadway; (ii) the minimum headway on the circulatory roadway t_{mc} and (iii) the minimum headway t_{fc} between two consecutive insertions (referred to as the *follow-up time*). Assuming a shifted exponential distribution of the headways:

$$p = q_c t_{mc} \text{ and } \tau = e^{t_{fc} q_c/(1-q_c t_{mc})} \left(\frac{1}{q_c} + \frac{t_{fc}}{e^{t_{fc} q_c/(1-q_c t_{mc})} - 1} \right)$$

Values of t_{mc} and t_{fc} will be given in the next section.

2.3.3. Micro-simulation model

In the chosen micro-simulation noise model, vehicle positions, speeds and accelerations used by the noise calculation process are output from a microscopic traffic flow model. This model is based on: (i) a *car-following algorithm* to simulate vehicle trajectories (Leclercq et al., 2007; Leclercq, 2007); (ii) an *insertion decision algorithm* to rule the merging or the crossing movements at intersections (Chevallier and Leclercq, 2008a,b). Compared to other classical micro-simulation tools listed by the Federal Highway Administration such as VISSIM, CORSIM, INTEGRATION, PARAMICS or SIMTRAFFIC, the chosen traffic flow model is able to represent relevant merging or crossing behaviors when the intersection is hindered by a congestion spilling back from downstream. See Chevallier and Leclercq (2008a) for more details on this point.

In this paper, the traffic flow model is greatly simplified since no congestion comes from downstream (i.e. the departure arms are never congested). The car-following algorithm reduces to Newell's model (Newell, 2002). It assumes that the velocity of any vehicle n at time t, v_n^t, only depends on the spacing s_n^t with its leader $n-1$. Its position at the next simulation time-step $t+\Delta t$, $x_n^{t+\Delta t}$, is given as the minimum between the position it is willing to reach (*free-flow term*) and the position it cannot overpass due to the downstream vehicle (*congested term*):

$$x_n^{t+\Delta t} = \min\left[\underbrace{x_n^t + \min(u, v_n^t + a(v_n^t)\Delta t)\Delta t}_{\text{free-flow term}}; \underbrace{(1-\alpha)x_{n-1}^t + \alpha x_{n-1}^t + v_{n-1}^t \Delta t - s_e(v_{n-1}^{t+\Delta t})}_{\text{congested term}}\right] \quad (5)$$

where $s_e(v) = s_0(w+v)/w$ is the equilibrium spacing corresponding to speed v in congestion; $\alpha = w\Delta t / s_0$ is a non-dimensional coefficient; w is the speed at which a queue spills back; s_0 is the minimum spacing when vehicles are stopped.
The free-flow speed u and the acceleration rate a are set equal to the values presented in section 2.1.3. To suite urban conditions we chose w=21.1km/h, s_0=5.9m. Stability of equation (5) is ensured when the Courant-Friedrich-Lewy's condition $\Delta t < s_0 / w$ is met. We set Δt=1s for convenience.

When there is no spillback phenomena, the insertion decision algorithm is simply a classical gap-acceptance algorithm. A non-priority vehicle is allowed to cross or merge into a priority stream if:

- the follow-up time t_{fc} (for the roundabout) or t_{ft} (for the signalized intersection) has elapsed since the previous non-priority vehicle has performed its manoeuvre;
- the next conflicting vehicle is beyond a distance d_{lag} from the conflict point.

The follow-up time aims at capturing the wasted time due to acceleration constraints. As the microscopic model already incorporates bounded acceleration in the free-flow term of equation (5), it is set equal to the minimum headway on the circulatory roadway $t_{fc} = t_{mc} = s_0(w+u_c)/(wu_c)$=2s or on the internal links of the signalized intersection

$t_{ft} = t_{mt} = s_0(w+u_t)/(wu_t)$ =2.3s. For the roundabout, to conform with classical entry capacity curves, we set $d_{lag} = u_c t_{mc}$ = 11.8m. For the signalized intersection, d_{lag} is computed as the product of the time needed to cross the opposite 3m-width road (which depends on the initial speed of the non-priority vehicle) with the speed of the next conflicting vehicle (which evolves in time if it is accelerating).

3. RESULTS

3.1. Roundabout case study: comparison of the traffic noise methodologies

For the roundabout scenario, the equivalent sound pressure levels $L_{Aeq,30\mathrm{mn}}$ obtained at all receptors during each 30mn-period are depicted in figure 5a. Whatever the traffic demand is, all models produce the same average noise levels far from the intersection, at reception points M_1 and M_{24} where all vehicles are running at constant free-flow speeds. Simple procedures like the static noise emission model are therefore sufficient to assess acoustic levels in homogeneous traffic. Yet, they are irrelevant closer to intersections. On the one hand, they predict erroneous noise levels since they disregard the junction layout. By neglecting the curvature of the circulatory roadway, the distance between receptors M_{12} and M_{13} and the road axis is longer than it should be. This induces an irrelevant decrease in sound pressure levels next to the central island. On the other hand, they fail in capturing spatial noise variations around the road crossing by disregarding single vehicle dynamics. Globally, the sound levels predicted by the static model remain constant. They are underestimated compared to the analytic or the micro-simulation models since full throttle conditions are not caught by the static method.

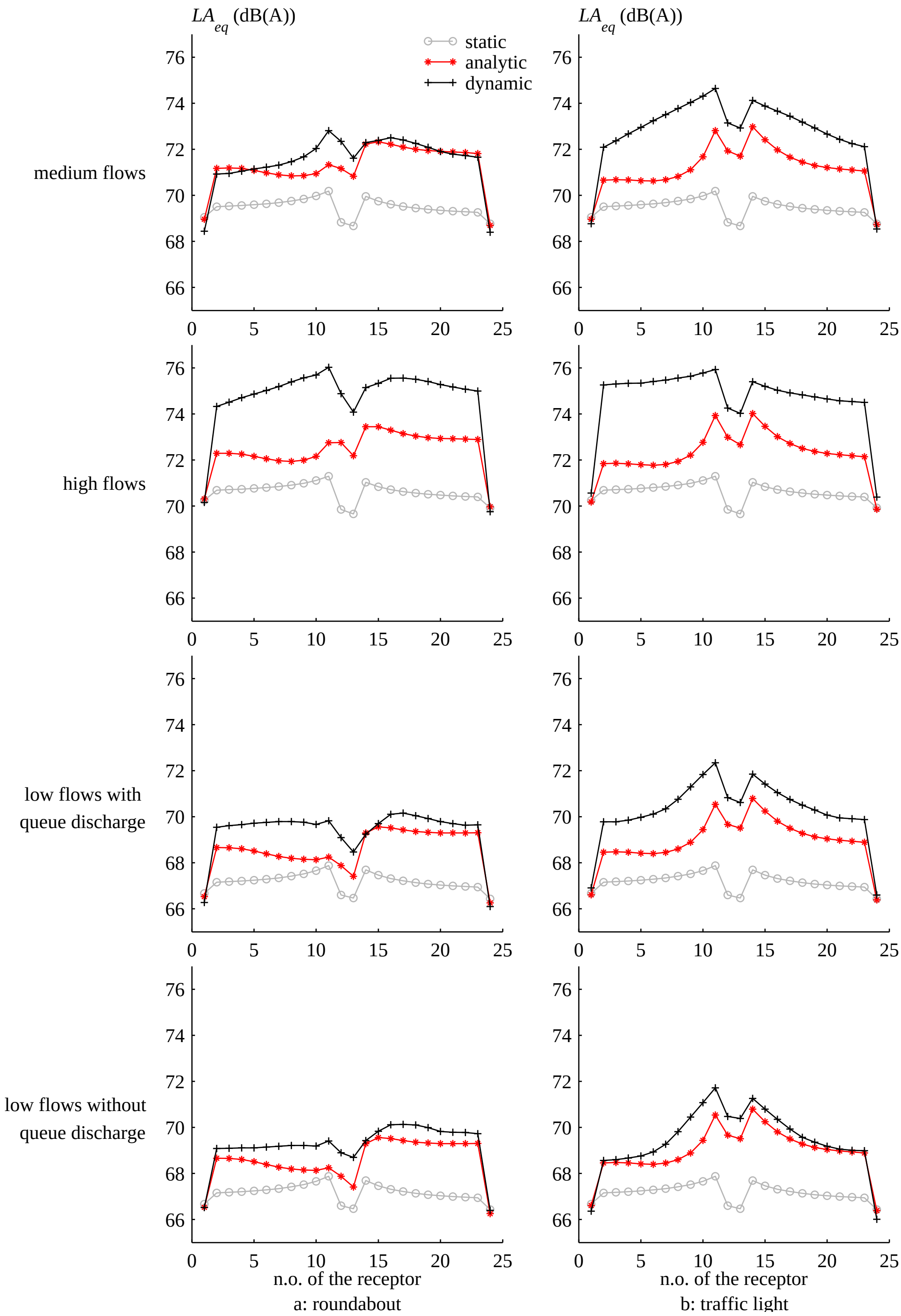

Fig.5. Predicted noise levels at the roundabout and the traffic light by different methodologies

By accounting for single vehicle dynamics, the analytic and micro-simulation noise models give similar noise variation trends. Firstly, they both predict a rise in noise emissions at receptors M_{10} and M_{11} which is triggered by stopping vehicles accelerating on the circulatory roadway to recover their maximum turning speed. Note that during the low traffic period this phenomena almost disappears since very few vehicles are disturbed at the conflict point. Secondly, they estimate lower noise levels at reception points M_{12} and M_{13} because of reduced speeds on the circulatory roadway. Finally, they both produce a noise increase at the

beginning of the departure links (see receptor M_{14}) due to accelerating vehicles leaving the roundabout. Notice that, sound emissions progressively decrease along the next 60m until all vehicles recover the free-flow speed.
Despite substantial agreement in noise variations, the absolute noise estimates given by the analytic and micro-simulation models are very different, especially when traffic flow dynamics has a substantial impact on sound emissions. The largest discrepancy between both models occurs in high traffic. Noise levels are 2.5dB(A) higher with the micro-simulation model since it fully captures the queues spilling back on the approaching links. Queuing vehicles accelerate and stop several times before entering the circulatory roadway. Since noise emissions are higher in full throttle conditions than in cruising mode at maximum speed (54km/h) (see figure 2a), the equivalent sound pressure levels at all reception points rise up. This increase in noise levels is more sticking than the one occurring with the analytic method which is due to the overestimation of traffic volumes (remind that analytic models neglect capacity restrictions in congestion). To a smaller extent, noise variations also affect the medium and low traffic periods. Along the approaching links, noise levels predicted by the analytic model tend to slightly lessen because of decelerating vehicles near the intersection. This phenomena is balanced in the micro-simulation model by the contribution of stop-and-go vehicles trapped into small transient queues before entering the circulatory roadway. Finally, it is worth noticing that, in low traffic, noise deviation between the analytic and the micro-simulation models is greater during the first 30mn-period than during the second one. Indeed, in the micro-simulation model, some vehicles are still queuing on the major road at the beginning of the first period until the queue formed during the peak period has totally discharged. This queue dissipation phenomena is not accounted for in the analytic model which reduces the noise emissions.

3.2. Traffic light case study: comparison of the traffic noise methodologies

Results for the traffic light scenario are illustrated in figure 5b. The equivalent sound pressure levels predicted by the static model are the same as in the roundabout scenario since this method disregards both geometric effects and single vehicle dynamics. With the analytic model, the increase in noise levels at receptors M_{10} and M_{11} is more striking than previously since the number of stopping vehicles is more important at the traffic light than at the roundabout. Sound levels in the vicinity of the intersection center, at receptors M_{12} and M_{13}, are still lower than at the entries or the exits. However, they exceed the levels received at the roundabout because of non-stopping vehicles which go through at maximum speeds during green. Again, deviations between the analytic and the micro-simulation results are greater during the first period of low traffic than during the second one because of the queue discharge time effect. One could have expected that during the last low traffic period, the analytic and micro-simulation models had produced the same outputs. Yet, as in the roundabout scenario, short transient queues modeled by the micro-simulation tool on the approaching arms, trigger an increase in noise levels (up to 1dB(A)) next to the junction center. This effect spreads out and amplifies during the medium traffic period since queues are longer and more sustainable. Particularly, noise variations between both methods are more than 2dB(A). In oversaturated conditions, sound level differences are maximum and reach the same levels as in the roundabout scenario (2.5dB(A)) since queues spill back up to receptor M_1.

3.3. Noise impacts of roundabouts and traffic lights

Since traffic dynamics was shown to greatly influence sound pressure levels close to a road crossing, the micro-simulation results were used to compare the noise contribution of roundabouts and signalized intersections. As depicted in figure 6, replacing a roundabout by a traffic light can induce higher noise levels (up to 2.5dB(A)) in low and medium traffic. In low traffic, the increase concentrates in the vicinity of the intersection because of: (i) a greater number of stopping vehicles; (ii) non-stopping vehicles during green going straight ahead at high velocity. In medium traffic, it spreads out around the intersection arms due to longer and systematic queues. As soon as saturation is reached, the noise contributions of roundabouts and signalized intersections become similar.

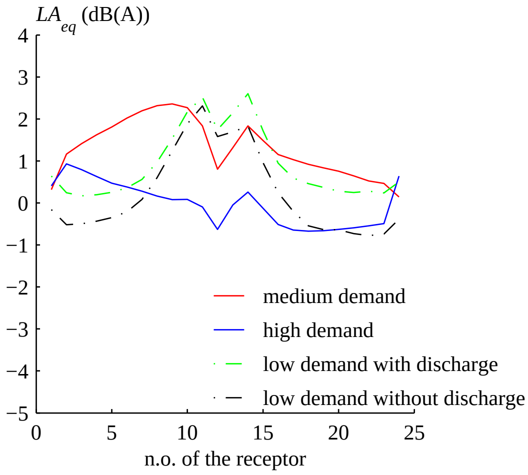

Fig.6. Noise abatement by transforming a signalized intersection into a roundabout

The noise impact comparison between both intersections can be refined through the analysis of the $L_{Aeq,1s}$ output by the micro-simulation model. In figure 7, the $L_{Aeq,1s}$ distributions, calculated at receptors M_1, M_7, M_{11} and M_{16}, are plotted for the whole 2h-simulation period and for each 30mn-period.

By averaging the $L_{Aeq,1s}$ frequencies over 2h, several peaks can be pinpointed:

- *free-flow speed peak*: at receptor M_1 or M_7, the peak at about 72dB(A) represents vehicles driving past the receptor at free-flow speed;
- *acceleration peak*: at receptors M_7, M_{11} and M_{16}, the right side peak at about 78dB(A) characterizes accelerating vehicles either trapped in a queue or leaving the intersection;
- *opposite side peak*: at receptor M_{16}, the peak at about 69dB(A) represents the effect of accelerating vehicles on the opposite side.

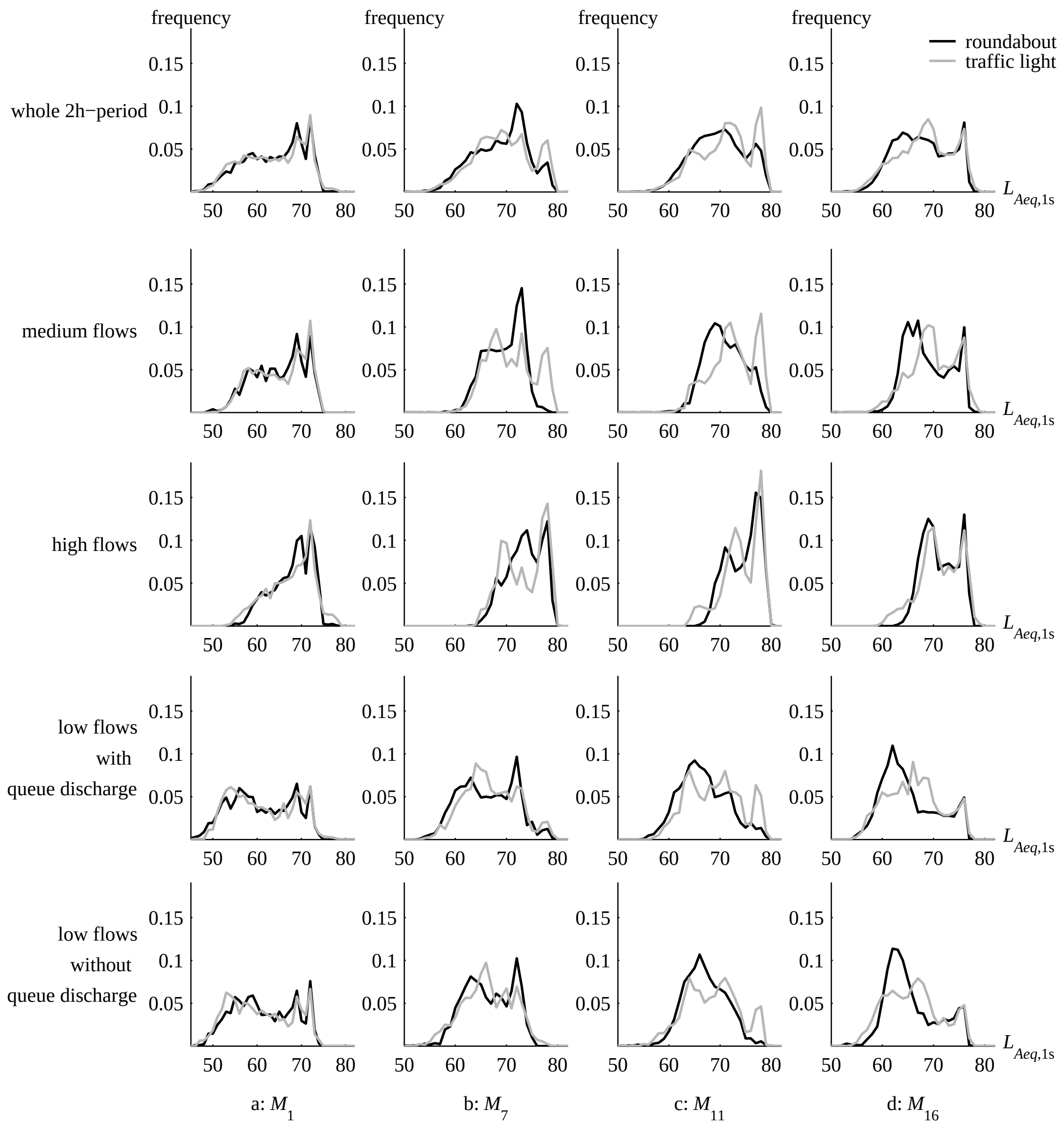

Fig.7. Distributions of the micro-simulated $L_{Aeq,1s}$ at four reception points

The frequency of those peaks vary with the traffic volume. It is also appealing to highlight how they evolve in space and differ from roundabouts to signalized intersections. Far from the junction, whatever the traffic demand, distributions are quite similar between both infrastructures. They are characterized by the free-flow speed peak which grows with traffic volume. This peak also occurs closer to the entry point, at receptor M_7, especially in low traffic. It coexists with the acceleration peak when congestion spills back on the approach arm. At roundabouts, the acceleration peak only occurs in high traffic volumes while it also affects the medium traffic period at signalized intersections (because of longer queues). It grows up at reception point M_{11} where all stopping vehicles are accelerating away from the entry lines. It sustains around the departure arms (see receptor M_{16}) until vehicles recover the free-flow speed. The opposite side peak appears at receptors M_{16} for both intersection types. In medium traffic, the value of this peak decreases for the roundabout case since vehicles on the opposite road stay in cruising conditions instead of stopping and the accelerating like at the signalized intersection. Finally, at all receptors and for both intersection type, the noise levels below 60dB(A) represent situations during which no vehicle is around the reception point. They are all the more frequent as the traffic volume is low. Because of queue formation at reception point M_7, they do not occur neither in medium nor in high traffic. The frequency of low levels is generally the same for both the roundabout and the signalized intersection except in high traffic at points M_{11} and M_{16}. In this case, the left tailed-distribution at the signalized intersection reveals that the discharge flow due to the traffic light is pulsed, contrary to the flow crossing the roundabout. Indeed, frequent low levels at around 62dB(A) occur when both signal phases are red: incoming vehicles are stopped and no exiting vehicle pass by the receptors.

3.4. Discussion

Static methods, which neglect geometric factors, changes in average kinematic patterns as well as traffic flow dynamics, are irrelevant to perform noise impact assessment near junctions. Furthermore, it seems hazardous to account for these phenomena by applying some ad-hoc corrective formula. Indeed, the discrepancy between the static and micro-simulation results is not only proportional to the traffic volumes or the distance to the intersection. It varies with the proportion of stopping vehicles, the average waiting-time and the stochastic queue evolution which are cumbersome to predict outside a traffic simulation tool.

Methods accounting for single vehicle dynamics appear to be more efficient in conducting noise impact appraisals at intersections. The highest noise levels at roundabouts and signalized intersections stand just downstream of the entry lines and at the beginning of the departure links because of accelerating vehicles. Yet, at junctions, most of accelerating phases stem from traffic flow dynamics which govern queue length formation and evolution. By explicitly catching these dynamic effects, micro-simulation models produce more relevant noise estimates. Although differences between analytic and micro-simulation outputs are moderate in low traffic (less than 1dB(A)), they go up with traffic demand. In medium traffic, the impact of short transient queues upstream of the conflict points can trigger a 1.5 dB(A) increase in noise levels that is not captured by the analytic model. Furthermore, in oversaturated conditions, noise levels rise up of more than 2.5dB(A) with the micro-simulation tool because of stop-and-go vehicles trapped into queues.

Another asset of micro-simulation models is to improve noise impact comparison between different kinds of junctions. By accounting for traffic flow dynamics, the estimated noise outputs are fully sensitive to the level of service of the road crossing layout. In light and medium traffic, replacing a signalized intersection by a roundabout can trigger a 2.5 dB(A) noise abatement. This result is in agreement with recent experimental studies (Berengier, 2002) or results found with another micro-simulator (De Coensel et al., 2006). The acoustic gain is triggered by: (i) lower velocities inside the junction, especially for non-disturbed through movements; (ii) a lower number of stop-and-go periods. To illustrate the second point, the average queue lengths on the major road given by the HCM formula (TRB, 2000) can be compared. It falls from 6.9 (respectively 14.2) vehicles at the signalized intersection to 1.3 (respectively 5.5) vehicles at the roundabout during the low (respectively the medium) traffic period. Better operating performance of roundabouts in undersaturated traffic conditions is therefore favorable with regard to acoustic patterns. In oversaturated conditions, both signalized intersections and roundabouts seem to have the same acoustical impact. Indeed, the traffic calming effect of roundabouts becomes negligible. Equivalent sound pressure levels are bounded by the emissions of stop-and-go vehicles on the congested approaching arms. The intersection type only influences the spatial extension of the highest noise levels which is linked to its capacity performance.

4. CONCLUSION

This paper has demonstrated that traffic dynamics have a substantial impact on noise levels at road crossings. Consequently, noise estimation procedures that only account for the geometric effects and single vehicle dynamics are not sufficient for conducting noise impact assessment at junctions. An efficient solution consists in using micro-simulation packages that couple a microscopic traffic simulation tool with noise emission laws and sound propagation algorithms. This allows for catching the noise impact of both intersection operation and intersection control device.

It could be valuable to complete this study by applying the tested methodologies to on-field measurements. Moreover, the sensitivity of the presented results to changes in noise emission laws should be worth investigating. Indeed, the engine-exhaust noise is expected to decrease for new vehicle fleets since engines are now cocooned with noise insulation. This will reduce vehicle emissions in full-throttle conditions. If they become lower than emissions at cruising free-flow speed, congested situations could induce noise abatement instead of increasing sound levels.

Acknowledgement

The authors would like to thank Cécile Bécarie for her careful and reactive contribution in the development of the micro-simulation package.

References

Berengier, M., 2002. Acoustical impact of traffic flowing equipments in urban areas. In Forum Acusticum, Sevilla, Spain.

Certu, 1980. French Guide for Transportation Noise (Guide du bruit des transports terrestres - Prévision des niveaux sonores). Ministère de l'environnement et du cadre de vie. 317p.

Chevallier, E. and Leclercq, L., 2008a. Macroscopic investigation of microscopic merging models at unsignalized intersections. In Transporation Research Board, Washington, DC, USA.

Chevallier, E. and Leclercq, L., 2008b. A microscopic dual-regime model for single-lane roundabouts. Submitted to Journal of Transportation Engineering.

De Coensel, B., De Muer, T., Yperman, I., and Botteldooren, D., 2005. The influence of traffic flow dynamics on urban soundscapes. Applied acoustics, 66(2):175-194.

De Coensel, B., Vanhove, F., Logghe, S., Wilmink, I., and Botteldooren, D., 2006. Noise emission corrections at intersections based on microscopic traffic simulation. In European Conference on Noise Control, Tampere, Finland.

Fleming, G., Rapoza, A., and Lee, C., 1995. Development of National Reference Energy Mean Emission Levels for the FHWA Traffic Noise Model, Version 1.0. Publication No. DOT-VNTSC-FHWA-96-2, Office of Engineering and Highway Operations Research and Development. 452p.

Goodman, P., 2001. The prediction of road traffic noise in urban areas. PhD thesis, Institute for Transport Studies, University of Leeds, UK.

Jonasson, H. and Storeheier, S., 2001. Nord 2000: New Nordic Prediction Method for Road Traffic Noise. SP Rapport 2001: 10, Swedish National Testing and Research Institute. 59p.

Leclercq, L., 2007. Hybrid approaches to the solutions of the Lighthill Whitham Richards model. Transportation Research Part B, 41(7):701-709.

Leclercq, L., Laval, J., and Chevallier, E., 2007. The Lagrangian coordinates and what it means for first order traffic models. In Allsop, R.E. and Bell, M. G. H. and Heydecker, B.G. (Ed.), Proceedings of the 17th International Symposium on Transportation and Traffic Theory, 735-753.

Leclercq, L. and Lelong, J., 2001. Dynamic evaluation of urban traffic noise. In Proceedings of the 17th International congress on Acoustics, Rome, Italy.

Makarewicz, R., Fujimoto, M., and Kokowski, P., 1999. A model of interrupted road traffic noise. Applied Acoustics, 57(2):129-137.

Makarewicz, R. and Golebiewski, R., 2007. Modeling of roundabout noise impact. Journal of the Acoustical Society of America, 122(2):860-868.

Menge, C., Rossano, C., Anderson, G., and Bajdek, C., 1998. FHWA Traffic Noise Model: Technical Manual. Publication No. DOT-VNTSC-FHWA-98-2, Office of Environment and Planning. 180p.

Newell, G., 2002. A simplified car-following theory: a lower-order model. Transportation Research Part B, 36(3):195-205.

Picaut, J., Bérengier, M., and Rousseau, E., 2005. Noise impact modelling of a roundabout. In International Congress and Exposition on Noise Control Engineering , Rio de Janeiro, Brazil.

RLS, 1990. Richtlinien für den Lärmschutz an Strassen. BM für Verkehr, Bonn, Germany.

Robinson, B., 2000. Roundabout: An Informational Guide. Publication No. FHWA-RD-00-067, www.tfhrc.gov.

Rodegerdts, L., 2004. Signalized intersections: Informational Guide. Publication No. FHWA-HRT-04-091, www.tfhrc.gov.

Stoilova, K. and Stoilov, T., 1998. Traffic noise and traffic light control. Transportation Research Part D, 3(6):399-417.

Suzuki, T., Tsukui, K., and Oshino, Y., 2003. Road traffic noise prediction model around signalized intersections. In International Congress and Exposition on Noise Control Engineering, Seogwipo, Korea.

TRB, 2000. Highway Capacity Manual. ISBN: 0-309-06746-4, National Academy of Sciences, Washington, DC, USA.

Volkmar, H., 2005. Development of a microscopic road traffic noise model for the assessment of noise reduction measures. In Final Conference, Berlin, Germany, www.rotranomo.com.

Wayson, R., MacDonald, J., Eaglin, R., and Wendling, B., 1997. Simulation approach to traffic noise modeling: American Automobile Manufacturers Association Community Noise Model Version 4.0. Transportation Research Record, 1601:64-70.

Yoshihisa, K., Oshino, Y., Yamamoto, K., and Tachibana, H., 2004. Road traffic noise prediction in the vicinity of signalized intersections in urban areas. In International Congress on Acoustics, Kyoto, Japan.